2808 *Inorg. Chem.* **2010**, *49*, 2808–2815
DOI: 10.1021/ic9021917

Inorganic Chemistry
Article

Interaction of $SbCl_5^{2-}$ and Thioether Groups at the Open Coordination Sites of Platinum(II) Diimine Complexes

Sayandev Chatterjee,[†] Jeanette A. Krause,[†] William B. Connick,*[,†] Caroline Genre,[‡] Alexandre Rodrigue-Witchel,[‡] and Christian Reber[‡]

[†]*Department of Chemistry, University of Cincinnati, P.O. Box 210172, Cincinnati, Ohio 45221-0172, and* [‡]*Département de Chimie, Université de Montréal, Montréal QC H3C 3J7, Canada*

Received November 5, 2009

In the solid-state, the approximately square planar cation in orange crystals of $[Pt(NO_2phen)(ttcn)](PF_6)_2$ (NO_2phen = 5-nitro-1,10-phenanthroline; ttcn = 1,4,7-trithiacyclononane) has a short apical Pt···S(ttcn) distance (2.9415(15) Å). In acetonitrile solution, the electronic spectrum shows a long-wavelength absorption band (412 nm; 2200 M^{-1} cm^{-1}), consistent with the notion that the axial Pt···S(ttcn) interactions stabilize states having metal-to-ligand charge-transfer (MLCT) character. Reaction with the hexachloroantimonate(V) salt of *tris*(4-bromophenyl)aminium ($TBPA^+$) results in complex redox chemistry, involving the platinum complex, $SbCl_5^{2-}$ and $TBPA^+$. In the case of $Pt(bpy)(ttcn)^{2+}$, orange-yellow crystals of $[Pt(bpy)(ttcn)]_2(Sb_4Cl_{16})$ were isolated from the reaction, whereas the reaction with $Pt(NO_2phen)(ttcn)^{2+}$ consistently yielded red crystals of $[Pt(NO_2phen)(ttcn)](SbCl_5)\cdot 2CH_3CN$. In the latter case, the geometry of the cation, including the apical Pt···S(ttcn) distance (2.9390(12) Å), is very similar to that of the PF_6^- salt. However, the basal plane of each square pyramidal $SbCl_5^{2-}$ opposes the nearly parallel coordination plane of an adjacent $Pt(NO_2phen)(ttcn)^{2+}$ complex, resulting in an unusually short intermolecular Pt···Sb distance of 3.4259(3) Å. The longest wavelength maximum in the diffuse reflectance spectrum and the solid-state emission maximum are shifted by ~1200 cm^{-1} and ~700 cm^{-1}, respectively, to the red of those of the PF_6^- salt, consistent with perturbation of the complex's electronic structure because of the Pt···Sb interaction.

Introduction

The interaction of a pendant nucleophile with the platinum(II) center at a vacant axial site of a square-planar complex with polypyridyl ligands can have a profound influence on electronic properties and reactivity.[1−8] For example, whereas $Pt(tpy)(phenyl)^+$ is not oxidized at < 1.3 V versus Ag/AgCl,[9] $Pt(tpy)(pip_2NCN)^+$ (Scheme 1) undergoes a nearly reversible two-electron oxidation at 0.4 V versus Ag/AgCl.[4,5] In the case of platinum(II) diimine complexes with a 1,4,7-trithiacyclononane ligand (ttcn), such as $Pt(bpy)(ttcn)^{2+}$, crystal structures show a close apical Pt···S contact that is significantly shorter than the sum of the van der Waals radii.[2,3,10,11] Substitution of the diimine chelate with other ligands (e.g., halides, phosphines) results in systematic variation in the apical Pt···S distance, which approximately correlates with the σ/π-donor properties of the ancillary ligands.[2] The formation of the apical Pt···S interaction in solutions of the diimine complexes results in rapid intramolecular exchange involving 1,4-metallotropic shifts of the ttcn ligand,[3] as well as a remarkable stabilization of excited states with metal-to-ligand charge-transfer (MLCT) character because of apical sulfur-to-platinum donation.[2] To further the understanding of the redox properties of $Pt(diimine)(ttcn)^{2+}$ systems,[12−14] we have recently undertaken an investigation of their reactions with the hexachloroantimonate(V) salt of *tris*(4-bromophenyl)aminium ($TBPA^+$), since $TBPA^+$ is a moderate oxidant (0.7 V vs ferrocene/ferrocenium in acetonitrile).[15] In the course of these

*To whom correspondence should be addressed. E-mail: bill.connick@uc.edu. Fax: (+1) 513-556-9239.

(1) Yip, J. H. K.; Suwarno; Vittal, J. J. *Inorg. Chem.* **2000**, *39*, 3537.
(2) Green, T. W.; Lieberman, R.; Mitchell, N.; Krause, J. A.; Connick, W. B. *Inorg. Chem.* **2005**, *44*, 1955.
(3) Nikol, H.; Bürgi, H.-B.; Hardcastle, K. I.; Gray, H. B. *Inorg. Chem.* **1995**, *34*, 6319.
(4) Jude, H.; Krause Bauer, J. A.; Connick, W. B. *J. Am. Chem. Soc.* **2003**, *125*, 3446.
(5) Jude, H.; Carroll, G. T.; Connick, W. B. *Chemtracts* **2003**, *16*, 13.
(6) Grant, G. J.; Spangler, N. J.; Setzer, W. N.; VanDerveer, D. G.; Mehne, L. F. *Inorg. Chim. Acta* **1996**, *246*, 31.
(7) Blake, A. J.; Gould, R. O.; Holder, A. J.; Hyde, T. I.; Lavery, A. J.; Odulate, M. O.; Schroder, M. *J. Chem. Soc., Chem. Commun.* **1987**, 118.
(8) Blake, A. J.; Holder, A. J.; Hyde, T. I.; Roberts, Y. V.; Lavery, A. J.; Schroder, M. *J. Organomet. Chem.* **1987**, *323*, 261.
(9) Hill, M. G.; Bailey, J. A.; Miskowski, V. M.; Gray, H. B. *Inorg. Chem.* **1996**, *35*, 4585.
(10) For example, see reference 2 and references therein.
(11) Janzen, D. E.; Mehne, L. F.; VanDerveer, D. G.; Grant, G. J. *Inorg. Chem.* **2005**, *44*, 8182.
(12) Grant, G. J.; Poullaos, I. M.; Galas, D. F.; VanDerveer, D. G.; Zubkowski, J. D.; Valente, E. J. *Inorg. Chem.* **2001**, *40*, 564.
(13) Grant, G. J.; Brandow, C. G.; Galas, D. F.; Davis, J. P.; Pennington, W. T.; Valente, E. J.; Zubkowski, J. D. *Polyhedron* **2001**, *20*, 3333.
(14) Grant, G. J.; Patel, K. N.; Helm, M. L.; Mehne, L. F.; Klinger, D. W.; VanDerveer, D. G. *Polyhedron* **2004**, *23*, 1361.
(15) Connelly, N. G.; Geiger, W. E. *Chem. Rev.* **1996**, *96*, 877.

 Published on Web 02/18/2010

Scheme 1. $Pt(tpy)(pip_2NCN)^+$ and $Pt(NO_2phen)(ttcn)^{2+}$

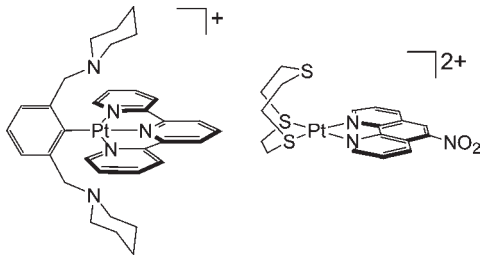

$Pt(pip_2NCN)(tpy)^+$ $Pt(NO_2phen)(ttcn)^{2+}$

studies, we were surprised to isolate $Pt(diimine)(ttcn)^{2+}$ salts with antimony(III)-containing counterions, indicating that $SbCl_6^-$ participates in the redox chemistry. In the case of $[Pt(NO_2phen)(ttcn)](SbCl_5)\cdot 2CH_3CN$, there is a close Sb···Pt contact, which, to our knowledge, is the first example of the interaction of the Sb(III) center of $SbCl_5^{2-}$ with a transition metal center.

Experimental Section

General Considerations. K_2PtCl_4 was obtained from Pressure Chemical (Pittsburgh, PA). 1,4,7-Trithiacyclononane (ttcn) was obtained from Aldrich Chemical Co. (Milwaukee, WI). All other reagents were obtained from Acros (Somerville, NJ). Acetonitrile for UV−visible absorption and electrochemical studies was distilled from calcium hydride. All other chemicals were used as received. $Pt(NO_2phen)Cl_2$ was prepared by the method reported for $Pt(phen)Cl_2$,[16] substituting NO_2phen for phen. $[Pt(NO_2phen)(ttcn)](PF_6)_2$ was prepared by a modification of a procedure for the preparation of bipyridyl analogues.[2] Elemental analysis was performed by Atlantic Microlab, Inc. (Norcross, GA). ^1H NMR spectra were recorded at room temperature using a Bruker AC 400 MHz instrument. Deuterated acetonitrile, acetone, and *N*,*N*-dimethylformamide (DMF) were obtained from Cambridge Isotope Laboratories (Andover, MA). ^1H NMR spectra are reported in parts per million (ppm) relative to $SiMe_4$ ($\delta = 0$ ppm) or relative to a protic solvent impurity in the case of CD_3CN ($\delta = 1.94$ for CD_2HN). Mass spectra were obtained by electrospray ionization of acetonitrile solutions using either an Ionspec HiRes ESI-FTICRMS instrument or a Micromass Q-TOF-II instrument.

UV−visible absorption spectra were recorded using a HP8453 Diode Array Spectrometer. Luminescence and Raman spectroscopy measurements were carried out using a Renishaw inVia imaging microscope system. Excitation sources were a 488 nm argon ion laser for luminescence experiments and a 785 nm diode laser for the Raman experiments. The microscope was used to focus the light onto a spot of approximately 1 μm in diameter and to collect the scattered light. The backscattered Raman light was detected with a Peltier cooled CCD detector. Sample temperatures were controlled with Linkam microscope cryostat between 80 and 300 K. All spectra were unpolarized and corrected for spectrometer response. Diffuse reflectance data were collected at 296 K using an Ocean Optics HR2000CG-UV-vis-NIR detector and a DH5000 light source. Samples for diffuse reflectance were prepared by grinding 10% by weight of the platinum complexes into TiO_2 using a mortar and pestle. A small amount of the mixture was placed on a microscope slide and pressed flat with another microscope slide before being inserted into the sample holder. Data were transformed to absorbance according to the equation Absorbance = −log (% reflectance).

Synthesis of $[Pt(NO_2phen)(ttcn)](PF_6)_2$. $[Pt(NO_2phen)(ttcn)](PF_6)_2$ was prepared by a modification of the method previously reported for the preparation of $[Pt(bpy)(ttcn)](PF_6)_2$,[2] substituting $Pt(bpy)Cl_2$ with $Pt(NO_2phen)Cl_2$. $Pt(NO_2phen)Cl_2$ (0.492 g, 1.0 mmol) and ttcn (0.180 g, 1.0 mmol) were refluxed in 30 mL of 1:1:1 methanol/acetonitrile/water for 3 h under argon. The solution was allowed to cool to room temperature, and excess NH_4PF_6 was added to precipitate an orange product. The orange powder was recrystallized from acetonitrile and ether to give orange crystals. The product is air-stable and soluble in polar organic solvents. Anal. Calcd for $C_{18}H_{19}F_{12}N_3O_2P_2PtS_3$: C, 24.28; H, 2.15; N, 4.72. Found: C, 24.26; H, 2.11; N, 4.83. ^1H NMR (CD_3CN, δ): 9.53 (1H,d), 9.36 (1H, d with Pt satellites, $J_{H-H} = 6$ Hz, $J_{H-Pt} = 24$ Hz), 9.34 (1H, d with Pt satellites, $J_{H-H} = 6$ Hz, $J_{H-Pt} = 24$ Hz), 9.25 (1H, s), 9.19 (1H, d), 8.27 (1H, dd), 8.25 (1H, dd), 3.23 (12H, m).

Reaction of $[Pt(NO_2phen)(ttcn)](PF_6)_2$ with TBPA($SbCl_6$). In a typical procedure, a solution of $[Pt(diimine)(ttcn)](PF_6)_2$ (0.009 g, 0.01 mmol) (diimine = NO_2phen or bpy) in 4 mL of acetonitrile was added to a solution of *tris*(4-bromophenyl)-aminium hexachloroantimonate (0.008 g, 0.01 mmol) in 4 mL of acetonitrile. The reaction was monitored by UV−visible absorption spectroscopy for as long as 39 days. For ^1H NMR experiments, deuterated acetonitrile was used (Supporting Information, Figure S1).

X-ray Crystallography. Orange crystals of $[Pt(NO_2phen)(ttcn)](PF_6)_2$ were obtained from CH_3CN-Et_2O. Insoluble orange-yellow crystals of $[Pt(bpy)(ttcn)]_2(Sb_4Cl_{16})$ and red insoluble crystals of $[Pt(NO_2phen)(ttcn)](SbCl_5)\cdot 2CH_3CN$ were reproducibly grown by very slow evaporation of the reaction mixtures described above; crystals typically formed within 30−50 days. Suitable single crystals for X-ray examination and data collection were mounted in a loop with paratone-N and transferred immediately to the goniostat bathed in a cold stream.

Intensity data for $[Pt(NO_2phen)(ttcn)](PF_6)_2$ and $[Pt(bpy)(ttcn)]_2(Sb_4Cl_{16})$ were collected at 193 K and 150 K, respectively, using a Bruker Platinum200 CCD detector at Beamline 11.3.1 at the Advanced Light Source (Lawrence Berkeley National Laboratory) with synchrotron radiation tuned to $\lambda = 0.77490$ Å. Intensity data for $[Pt(NO_2phen)(ttcn)](SbCl_5)\cdot 2CH_3CN$ were collected at 100 K using a Bruker SMART6000 CCD diffractometer with graphite-monochromated Cu Kα radiation, $\lambda = 1.54178$ Å. The data frames were collected using either APEX2 or SMART and processed using SAINT. Absorption and beam corrections were applied to the data using SADABS.

The structures were solved by a combination of direct methods in SHELXTL and the difference Fourier technique and refined by full-matrix least-squares on F^2. Non-hydrogen atoms were refined with anisotropic displacement parameters with the exception of the disordered F-atoms (F11A, F11B, F12A, F12B) for the PF_6^- counterion of $[Pt(NO_2phen)(ttcn)](PF_6)_2$. F11A, F11B, F12A, F12B were refined with a two-component disorder model (major occupancy set at 55%). The NO_2 group of $[Pt(NO_2phen)(ttcn)](PF_6)_2$ is disordered, and the major conformer refines to 64% occupancy. The anisotropic displacement parameters of the minor conformer were set to be equivalent to the better-behaved major conformer. Restraints were applied to the minor conformer (N3B−O3B, N3B−C7, N3B−C6 and N3B−C8) so that the geometry was consistent with typical NO_2 groups. H-atom positions were calculated and treated with a riding model; isotropic displacement parameters were defined as a^*U_{eq} of the adjacent atom ($a = 1.5$ for the solvent H-atoms and 1.2 for all others). For $[Pt(NO_2phen)(ttcn)](SbCl_5)\cdot 2CH_3CN$, the largest two residual electron density peaks appear in the vicinity of the NO_2 group. The refinements converged with crystallographic agreement factors summarized in Table 1.

Packing indices were calculated for $[Pt(NO_2phen)(ttcn)](PF_6)_2$ and $[Pt(NO_2phen)(ttcn)](SbCl_5)\cdot 2CH_3CN$ using the program PLATON. In the case of $[Pt(NO_2phen)(ttcn)](SbCl_5)\cdot 2CH_3CN$, the packing index was calculated first with the two

(16) Morgan, G. T.; Burstall, F. H. *J. Chem. Soc.* **1934**, 965.

Table 1. Crystal and Structure Refinement Data

	$[Pt(NO_2phen)(ttcn)](PF_6)_2$	$[Pt(NO_2phen)(ttcn)](SbCl_5).\ 2CH_3CN$	$[Pt(bpy)(ttcn)]_2(Sb_4Cl_{16})$
formula	$[C_{18}H_{19}N_3O_2S_3Pt](PF_6)_2$	$[C_{18}H_{19}N_3O_2S_3Pt]SbCl_5.2CH_3CN$	$[C_{16}H_{20}N_2S_3Pt]_2Sb_4Cl_{16}$
crystal System	triclinic	monoclinic	triclinic
space group	$P\bar{1}$	$P2_1/n$	$P\bar{1}$
a, Å	11.400(2)	13.2936(2)	10.9771(9)
b, Å	11.580(2)	15.2335(2)	11.7655(10)
c, Å	12.008(2)	15.1545(2)	12.3481(10)
α, deg	68.08(3)	90	104.751(1)
β, deg	62.99(3)	90.965(1)	95.230(1)
γ, deg	80.31(3)	90	109.032(1)
V, Å^3, Z	1310.2(5), 2	3068.47(7), 4	1431.2(2), 1
ρ_{calcd} (g cm^{-3})	2.257	2.125	2.457
μ, mm^{-1}	7.232	21.571	9.616
T, K	193(2)	100(2)	150(2)
reflns collected	16848	25703	16259
ind reflns, R_{int}	6416, 0.0483	5510, 0.0308	7053, 0.0334
$R1/wR2$ [$I > 2\sigma(I)$]	0.0379/ 0.1007	0.0296/ 0.0713	0.0271/ 0.0706
$R1/wR2$ (all data)	0.0392/ 0.1016	0.0313/ 0.0722	0.0289/ 0.0717

CH_3CN solvent molecules accounted for in the refinement. The packing index was calculated to be ~73.1% for the unit cell with no residual solvent accessible voids. The calculation was subsequently repeated but with the contribution of the two CH_3CN molecules removed from the refinement. It was found that the total potential solvent area volume is ~628 Å^3 (20.5% of the total unit cell volume) and a packing index of ~61.7%. Unfortunately PLATON does not handle disordered atoms when packing index calculations are desired. So for $[Pt(NO_2phen)(ttcn)](PF_6)_2$, the PF_6^- counterion was treated with the six F-atoms at 100% occupancy, the minor NO_2 disorder component was removed, and the major component of the NO_2 group was refined with 100% occupancy. The resulting packing index is ~73.4% with no residual solvent accessible voids.

Results and Discussion

Synthesis and Spectroscopy. $Pt(NO_2phen)(ttcn)^{2+}$ was prepared by refluxing $Pt(NO_2phen)Cl_2$ with ttcn in 1:1:1 MeCN-MeOH-H_2O for 3 h. Subsequent metathesis of the chloride product with excess NH_4PF_6 yielded the hexafluorophosphate salt. Orange crystals of the complex were obtained by vapor diffusion of ether into an acetonitrile solution. The identity of the product was confirmed by elemental analysis, mass spectrometry and X-ray crystallography. The ^{1}H NMR spectrum in CD_3CN shows the expected pattern of seven aromatic proton resonances, as well as a multiplet centered around 3.23 ppm consistent with the ttcn ligand being fluxional.[3]

In acetonitrile solution, the complex exhibits a broad long-wavelength absorption band at 412 nm (2200 M^{-1} cm^{-1}), having significant MLCT[d(Pt)→diimine(π^*)] character. The band occurs at longer wavelengths than expected for a platinum(II) diimine complex with two thioether donor groups, and this observation is consistent with the notion that the axial Pt···S(ttcn) interactions persist in solution and contribute >0.4 eV to the stabilization of $Pt(diimine)(ttcn)^{2+}$ MLCT states.[2] Shortening the axial Pt···S(ttcn) distance is expected to destabilize the metal d levels because of electron repulsion and thereby lower the energies of MLCT states. The absorption maximum is shifted to the red by 850 cm^{-1} from that of $Pt(bpy)(ttcn)^{2+}$ and 800 cm^{-1} from that of $Pt(phen)(ttcn)^{2+}$. This result illustrates the synergistic influence of diimine substituents and the apical Pt···S interactions on the energies of MLCT states of $Pt(diimine)(ttcn)^{2+}$ complexes, as previously suggested for bipyridyl ligands.[2] The observed shifts are noticeably smaller for ruthenium(II) and rhenium(I) diimine complexes, whose spectroscopic properties often correlate well with those of platinum(II) polypyridyl systems. For example, the MLCT absorption maxima of $Ru(NO_2phen)(NH_3)_4^{2+}$, $Ru(phen)_2(NO_2phen)^{2+}$, and $Ru(bpy)_2(NO_2phen)^{2+}$ are shifted to the red of those of $Ru(bpy)(NH_3)_4^{2+}$, $Ru(bpy)_2(phen)^{2+}$, and $Ru(phen)_3^{2+}$ by 300, −300, and > −50 cm^{-1}, respectively.[17−21] For an analogous pair of $Re(L)(CO)_3Cl$ complexes (L = phen, NO_2phen), the nitro group is responsible for a 140 cm^{-1} red shift in the MLCT absorption band maximum.[22] For the $Pt(L)(CCPh)_2$ (L = phen, NO_2phen) pair, the shift is 300 cm^{-1}.[23] These observations can be understood by noting that introduction of electron-withdrawing groups on a diimine ligand stabilizes the ligand π^* level, which contributes to the stabilization of MLCT states. However, electron-withdrawing substituents also reduce the donor capacity of the diimine ligand, and this effect tends to lower the energies of the metal d orbitals, which contributes to the destabilization of MLCT states. As a consequence, the influence of substituents is somewhat less than expected from solely considering the changes in energy of the ligand π^* orbital. In the case of the $Pt(diimine)(ttcn)^{2+}$ systems, electron withdrawing substituents on the diimine ligand enhance metal acidity and increase the axial Pt···S(ttcn) interaction. This interaction will tend to compensate for the reduced diimine donor capacity through sulfur-to-platinum electron donation. In other words, the axial Pt···S(ttcn) interaction reinforces the tendency of diimine electron-accepting substituents to stabilize MLCT states, as well as the tendency of electron-releasing substituents to destabilize MLCT states.

Reactivity. To investigate the oxidation chemistry of $Pt(NO_2phen)(ttcn)^{2+}$, an acetonitrile solution of the complex was treated with 1 equiv of *tris*(4-bromophenyl)aminium ($TBPA^+$) hexachloroantimonate(V). Upon

(17) McDevitt, M. R.; Ru, Y.; Addison, A. W. *Transition Met. Chem.* **1993**, *18*, 197.
(18) Ye, B.-H.; Chen, X.-M.; Zeng, T.-X.; Ji, L.-N. *Inorg. Chim. Acta* **1995**, *240*, 5.
(19) Ye, B.-H.; Ji, L.-N. *Transition Met. Chem.* **1999**, *24*, 8.
(20) Mines, G. A.; Roberts, J. A.; Hupp, J. T. *Inorg. Chem.* **1992**, *31*, 125.
(21) Ando, I.; Ishimura, D.; Ujimoto, K.; Kurihara, H. *Inorg. Chem.* **1996**, *35*, 3504.
(22) Wrighton, M.; Morse, D. L. *J. Am. Chem. Soc.* **1974**, *96*, 998.
(23) Hissler, M.; Connick, W. B.; Geiger, D. K.; McGarrah, J. E.; Lipa, D.; Lachicotte, R. J.; Eisenberg, R. *Inorg. Chem.* **2000**, *39*, 447.

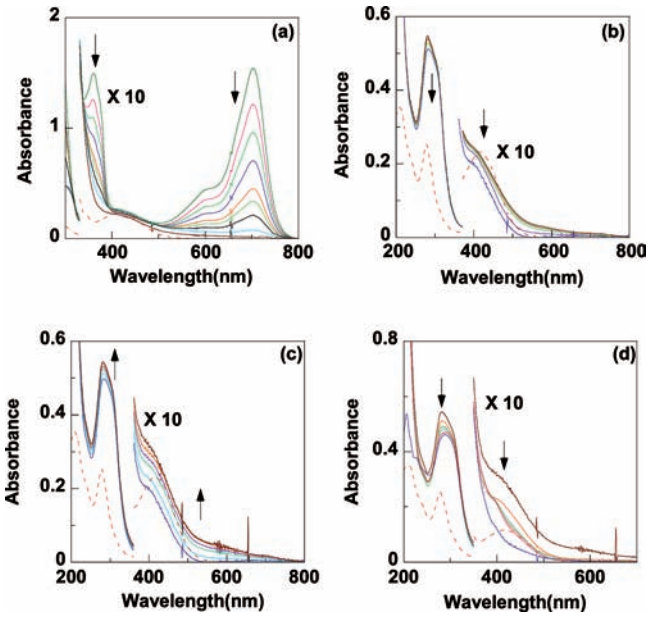

Figure 1. UV−visible absorption spectra recorded after combining equal volumes of 10^{-5} M [Pt(NO_2phen)(ttcn)](PF_6)$_2$ with 10^{-5} M TBPA($SbCl_6$) in CH_3CN: (a) 1−30 min. (brown line), (b) 30 min to 6 h. (30 min, brown line; 6 h., blue line), (c) 6−12 h. (6 h., blue line; 12 h., brown line), and (d) 12−48 h. (12 h, brown line; 48 h, orange line; 39 days, blue line). The spectrum of 10^{-5} M [Pt(NO_2phen)(ttcn)](PF_6)$_2$ (dashed red line) is shown in each panel for comparison.

dissolution of TBPA($SbCl_6$), the yellow solution immediately turned an intense blue color characteristic of $TBPA^+$. Over a period of 10 min, the color gradually turned increasingly green until finally becoming yellow. Full determination of the products and mechanism of this reaction is the subject of ongoing investigations; however, the data accumulated thus far are consistent with rapid reduction of $TBPA^+$ and slower reduction of $SbCl_6^-$ by platinum(II). For example, UV−visible absorption spectra recorded after the addition of oxidant confirm the gradual disappearance of the $TBPA^+$ absorption maxima near 360 and 700 nm; the intensity at 700 nm reaches 90% of its initial value within 30 min (Figure 1a). Over the same time period, solutions of TBPA($SbCl_6$) are stable, indicating that the platinum complex is involved in the reduction of $TBPA^+$. Over of the next 5.5 h, changes in the absorption spectrum are relatively small (Figure 1b). For comparison, ^{1}H NMR spectra recorded within 5 min of mixing exhibit a single set of NO_2phen proton resonances and overlapping broadened ttcn resonances (Supporting Information, Figure S1). Both sets of resonances are shifted downfield from those of Pt(NO_2phen)(ttcn)$^{2+}$, as might be expected in the presence of paramagnetic species. During the first 30 min, these resonances appear to lose intensity relative to the residual solvent and gradually shift back toward those of Pt(NO_2phen)(ttcn)$^{2+}$. There is a simultaneous appearance of broadened TBPA resonances. After ~6 h, the TBPA resonances are reasonably sharp, and the NO_2phen and ttcn proton resonances, though slightly broadened, match those of Pt(NO_2phen)(ttcn)$^{2+}$, albeit ~0.7 as intense as in the spectrum recorded at 5 min. Interestingly, no other identifiable product resonances were observed, but formation of paramagnetic NO_2phen/ttcn-containing products cannot be ruled out.

Scheme 2. Reactions of [Pt(NO_2phen)(ttcn)](PF_6)$_2$ and [Pt(bpy)(ttcn)](PF_6)$_2$ with TBPA($SbCl_6$) in Acetonitrile Solution

$$[Pt(NO_2phen)(ttcn)](PF_6)_2 \xrightarrow[CH_3CN]{TBPA(SbCl_6)} [Pt(NO_2phen)(ttcn)](SbCl_5).2CH_3CN \quad (red\ crystals)$$

$$[Pt(bpy)(ttcn)](PF_6)_2 \xrightarrow[CH_3CN]{TBPA(SbCl_6)} [Pt(bpy)(ttcn)]_2(Sb_4Cl_{16}) \quad (yellow\ crystals)$$

From 6 to 12 h after initial mixing, there is an increase in absorbance in the 360−700 nm region, which notably includes wavelengths where TBPA and antimony halide complexes do not typically absorb strongly (Figure 1c). At longer times, there is a gradual decrease in absorbance at $>$360 nm. After several weeks, the spectrum ceases to change, and absorbance in the region of the MLCT band is substantially diminished from its initial value. Spectroelectrochemical measurements of Pt(diimine)(ttcn)$^{2+}$ complexes have established that loss of absorbance in the vicinity of the MLCT band is characteristic of oxidation to platinum(IV),[24] which is consistent with the expectation that MLCT states are strongly destabilized by metal oxidation.

Similarly, ^{1}H NMR spectra only begin to show evidence of diamagnetic NO_2phen/ttcn-containing products ~2 days after initial mixing. The identity of the platinum-containing products is not certain. ESI-mass spectra of reaction solutions are consistent with platinum(II) fragments and therefore have not provided direct evidence of oxidized platinum products. Upon allowing solutions of Pt(NO_2phen)(ttcn)$^{2+}$ and TBPA($SbCl_6$) to slowly evaporate over the course of 30−50 days, we have consistently been able to isolate small quantities of insoluble dark red needle-shaped crystals of the platinum(II) salt [Pt(NO_2phen)(ttcn)]($SbCl_5$)·2CH_3CN, and this product is the main focus of this report (Scheme 2). These observations confirm that the antimony(V) anion also is reduced. It is worth noting that there is some precedent for oxidation of metal complexes and organic substrates by $SbCl_6^-$ to give Sb(III) products, though the mechanisms have not been fully resolved.[25−27] To investigate this possibility, we treated a solution of Pt(NO_2phen)(ttcn)$^{2+}$ with $SbCl_5$. The MLCT band loses intensity, but the reaction occurs at least 100 times more slowly than with $TBPA^+$ (Supporting Information, Figure S2). Given the increased chloride donor capacity of $SbCl_6^-$ as compared to $SbCl_5$ and the availability of an open coordination site on the platinum(II) center, it is not unreasonable that the reaction with $SbCl_6^-$ is more rapid.

Spectroscopy. Interestingly, crystals of [Pt(NO_2phen)(ttcn)]($SbCl_5$)·2CH_3CN are a noticeably darker red color than those containing Pt(NO_2phen)(ttcn)](PF_6)$_2$. Diffuse reflectance spectra confirm the differences in absorption properties of the two salts (Figure 2a). The PF_6^- salt shows a lowest energy band maximum near 435 nm. The band is shifted by ~1300 cm^{-1} to the red of the MLCT solution absorption band, likely as a consequence of the

(24) Chatterjee, S.; Grove, L. J.; Krause, J. A.; Connick, W. B. manuscript in preparation.
(25) Ohta, A.; Yamashita, Y. *Mol. Cryst. Liq. Cryst.* **1997**, *296*, 1.
(26) Cowell, G. W.; Ledwith, A.; White, A. C.; Woods, H. J. *J. Chem. Soc. B* **1970**, 227.
(27) Bott, S. G.; Brammer, L.; Connelly, N. G.; Green, M.; Orpen, A. G.; Paxton, J. F.; Schaverien, C. J. *J. Chem. Soc., Dalton Trans.* **1990**, 1957.

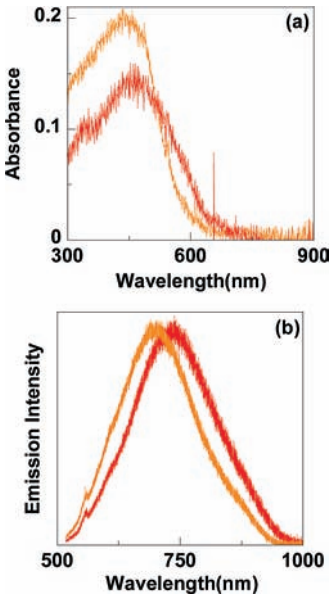

Figure 2. (a) Diffuse reflectance spectra (10% by weight of the ground complex in TiO_2) and (b) single-crystal emission spectra of $[Pt(NO_2phen)(ttcn)](PF_6)_2$ (orange line) and $[Pt(NO_2phen)(ttcn)](SbCl_5)\cdot 2CH_3CN$ (red line).

restricted position of the axial sulfur atom in the solid state. The maximum in the spectrum of the $SbCl_5^{2-}$ salt occurs near 465 nm, shifted by ~1200 cm^{-1} to the red of that of the PF_6^- crystals. Both complexes exhibit broad (fwhm ~4,000 cm^{-1}) and nearly symmetric emission bands (PF_6^-, 700 nm; $SbCl_5^{2-}$, 735 nm; Figure 2b). Comparison with emissions from other antimony(III) chloride salts ($\lambda_{max} < 640$ nm),[28] confirms that the observed luminescence does not originate from $SbCl_5^{2-}$. In analogy to related complexes,[2] we assign the emissions to a lowest excited state having significant MLCT character involving the platinum center and the phenanthrolinyl ligand. The red shift of the absorption and emission features of the $SbCl_5^{2-}$ salt is suggestive of intermolecular interactions involving the $Pt(NO_2phen)(ttcn)^{2+}$ complex, though the symmetrical band shape and broadness are somewhat inconsistent with either π-stacking interactions or short Pt···Pt interactions.[29−31] For comparison, subjecting $Pt(bpy)(ttcn)^{2+}$ to the same treatment with TBPA-($SbCl_6$) yielded orange-yellow crystals of $[Pt(bpy)(ttcn)]_2$-(Sb_4Cl_{16}), which are indistinguishable in color from crystals of $[Pt(bpy)(ttcn)](PF_6)_2$ (Scheme 2).

The Raman spectra, presented in the Supporting Information, Figure S3, clearly show the peaks assigned in the literature[32−35] to the totally symmetric stretching modes of the PF_6^- and $SbCl_5^-$ anions. The totally symmetric stretching mode for PF_6^- is observed at 760 cm^{-1} identical within experimental precision to the literature value of 756 cm^{-1}.[35] Significant differences are observed for the $SbCl_5^-$ stretching frequencies, observed as a broad Raman peak with a maximum at 311 cm^{-1}, extending from 280 cm^{-1} to 330 cm^{-1}. Literature stretching frequencies for the $Sb-Cl_{axial}$ mode are[32] 356 cm^{-1} and[33] 445 cm^{-1}, higher in frequency than the range of Raman shifts covered by the broad peak. Stretching frequencies of[32] 307 cm^{-1} and[33] 285 cm^{-1} have been reported for the $Sb-Cl_{equatorial}$ mode, both values in the range covered by the prominent peak in our experimental spectrum. A recent Raman study on a series of $SbCl_5$-Lewis base complexes reports experimental frequencies of 355 cm^{-1} and 302 cm^{-1} for the $Sb-Cl_{axial}$ and $Sb-Cl_{equatorial}$ modes, respectively.[34] These comparisons identify an unusually low $Sb-Cl_{axial}$ frequency in our compound, as qualitatively expected in the presence of significant Sb−Pt interactions.

Crystal Structures. The preceding observations prompted the determination of the structures of the PF_6^- and $SbCl_5^{2-}$ salts of $Pt(NO_2phen)(ttcn)^{2+}$, as well as the $Sb_4Cl_{16}^{4-}$ salt of $Pt(bpy)(ttcn)^{2+}$. Oak Ridge thermal-ellipsoid plot (ORTEP) images are shown in Figure 3, and important distances and angles are collected in Table 2. For each structure, the diimine and ttcn ligands of the cation bond in a bidentate fashion to the Pt atom. The ttcn ligand adopts an endodentate geometry, with the third sulfur atom (S3) forming a characteristically short axial Pt···S3 interaction (PF_6^-, 2.9415(15); $SbCl_5^{2-}$, 2.9390(12); $Sb_4Cl_{16}^{4-}$, 2.9944(10) Å) that is shorter than the sum of the van der Waals radii (< 3.55 Å).[36] Thus, the coordination geometry of the cations is slightly pyramidally distorted. The anions and cations pack as discrete units, and in the case of the PF_6^- salt, there are no unusually short intermolecular interactions. The nitro group exhibits typical two-site disorder bonding to either C6 or C7.

For both the PF_6^- salt and $Sb_4Cl_{16}^{4-}$ salts, the Pt-(diimine)$(ttcn)^{2+}$ cations pack in pairs in a head-to-tail arrangement with the approximately planar diimine ligands at the interface and the dangling S3 groups on opposing sides. However, the diimine ligands are well separated, and the intermolecular spacings between best-fit planes (PF_6^-, 3.59; $Sb_4Cl_{16}^{4-}$, 3.52 Å) do not suggest significant π-interaction. Somewhat similar packing arrangements occur for the phen and 4,4′-dimethyl-2,2′-bipyridine derivatives.[2,3] For the PF_6^- salt, there is significant asymmetry in several bond length pairs, including: S1−C13 (1.794(8) Å) and S2−C14 (1.856(8) Å) and C2−C3 (1.319(13) Å) and C10−C11 (1.377(11) Å). These differences correlate well with the short intermolecular contacts involving these atoms or bonded hydrogen atoms (H10···F7, 2.46; H10···F10, 2.39, H11···F4, 2.65; S2···O1A, 3.142(17); S2···O1B, 3.249(32); C13···F6, 3.103(9); C14···O2A, 3.195(12) Å). For the $Sb_4Cl_{16}^{4-}$ salt, the bipyridyl ligand is somewhat bowed, resulting in an root mean square deviation of 0.096 Å from the best-fit plane. This appears to be a consequence of short intermolecular contacts between the $Sb_4Cl_{16}^{4-}$ anion and the α-carbon atoms of the bpy ligand (C1···Cl5, 3.343(4); C10···Cl7, 3.343(4) Å). We know

(28) Petrochenkova, N. V.; Storozhuk, T. V.; Mirochnik, A. G.; Karasev, V. E. *Russ. J. Coord. Chem.* **2002**, *28*, 501.
(29) Miskowski, V. M.; Houlding, V. H. *Inorg. Chem.* **1989**, *28*, 1529.
(30) Miskowski, V. M.; Houlding, V. H.; Che, C.-M.; Wang, Y. *Inorg. Chem.* **1993**, *32*, 2518.
(31) Bailey, J. A.; Hill, M. G.; Marsh, R. E.; Miskowski, V. M.; Schaefer, W. P.; Gray, H. B. *Inorg. Chem.* **1995**, *34*, 4591.
(32) Wilmshurst, J. K. *J. Mol. Spectrosc.* **1960**, *5*, 343.
(33) Szymanski, H. A.; Yelin, R.; Marabella, L. *J. Chem. Phys.* **1967**, *47*, 1877.
(34) Klapötke, T. M.; Nöth, H.; Schütt, T.; Suter, M.; Warchold, M. *Z. Anorg. Allg. Chem.* **2001**, *627*, 1582.
(35) Heyns, A. M. *Spectrochim. Acta* **1977**, *33A*, 315.
(36) Bondi, A. *J. Phys. Chem.* **1964**, *68*, 441.

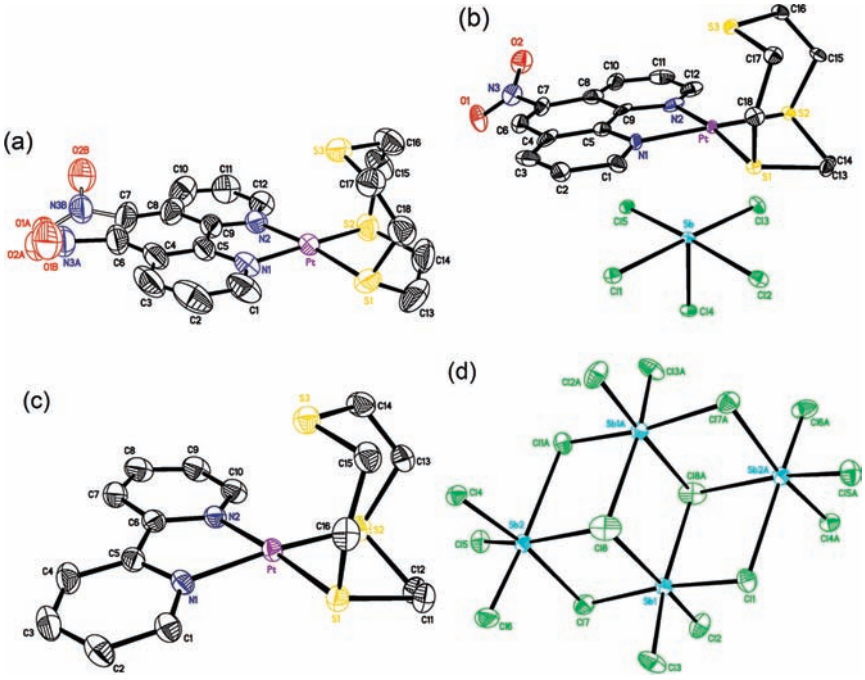

Figure 3. ORTEP diagrams of the (a) cation in $[Pt(NO_2phen)(ttcn)](PF_6)_2$, (b) the cation and anion in $[Pt(NO_2phen)(ttcn)](SbCl_5)\cdot 2CH_3CN$, as well as (c) the cation and (d) anion in $[Pt(bpy)(ttcn)]_2(Sb_4Cl_{16})$. H-atoms are omitted for clarity, thermal ellipsoids at 50% probability.

Table 2. Selected Distances (Å) and Angles (deg) for $[Pt(NO_2phen)(ttcn)](PF_6)_2$, $[Pt(NO_2phen)(ttcn)](SbCl_5)\cdot 2CH_3CN$, and $[Pt(bpy)(ttcn)]_2(Sb_4Cl_{16})$

	$[Pt(NO_2phen)(ttcn)](PF_6)_2$	$[Pt(NO_2phen)(ttcn)](SbCl_5)\cdot 2CH_3CN$	$[Pt(bpy)(ttcn)]_2(Sb_4Cl_{16})$
Pt−N1	2.064(5)	2.071(4)	2.044(3)
Pt−N2	2.061(4)	2.059(4)	2.043(3)
Pt−S1	2.2696(17)	2.2825(11)	2.2585(9)
Pt−S2	2.2698(18)	2.2585(11)	2.2549(9)
Pt−S3	2.9415(15)	2.9390(12)	2.9944(10)
N1−Pt−N2	80.03(19)	80.14(19)	79.75(13)
N2−Pt−S1	173.18(12)	171.78(13)	175.30(9)
N1−Pt−S1	95.28(15)	95.75(14)	95.86(9)
N2−Pt−S2	95.57(14)	94.99(14)	95.28(9)
N1−Pt−S2	174.09(13)	174.33(13)	169.37(8)
S1−Pt−S2	88.74(7)	88.72(4)	88.77(3)

of only five other examples of structurally characterized salts with discrete $Sb_4Cl_{16}^{4-}$ anions,[37−42] and in crystals of $[Pt(bpy)(ttcn)](Sb_4Cl_{16})$, the anion adopts a regular cubane geometry, similar to that found for $[dppf]_4(Sb_4Cl_{16})$. EtOH (dppf = bis(diphenylphosphino)ferrocene),[37] $[Me_2EtPhN]_4(Sb_4Cl_{16})$[38] and $(PT)(Sb_4Cl_{16})$ (PT = phenothiazine)[39] It lies on an inversion center and has two crystallographically distinct Sb atoms, Sb1 and Sb2, in distorted octahedral Cl atom environments. Each Sb1 octahedron shares an edge with three other octahedra in the cluster and has two terminal Sb−Cl bonds. Each Sb2 octahedron shares an edge with two other octahedra in the cluster and has three terminal Sb−Cl bonds. Consequently, the cluster is held together by four three-center Cl-bridged bonds and two four-center Cl-bridged bonds. The average of the terminal Sb−Cl bond lengths (2.407(30) Å) is in excellent agreement with the average (2.412(26) Å) of those for the three previously reported structures. The Sb−Cl distances in the two-center (2.53−3.13 Å) and 3-center bridge bonds (3.05−3.15 Å) fall within the ranges of previously reported values for similar anions (2.46−3.50 Å and 2.87−3.23 Å, respectively).[37−39]

In the case of $Pt(NO_2phen)(ttcn)](SbCl_5)\cdot 2CH_3CN$, the basal plane of each square pyramidal $SbCl_5^{2-}$ opposes the basal plane of an adjacent $Pt(NO_2phen)(ttcn)^{2+}$ pyramid. The coordination planes defined by the four equatorial atoms bonded to Sb and Pt, respectively, are nearly parallel, resulting in an unusually short intermolecular Pt···Sb distance of 3.4259(3) Å. To our knowledge, this is the first example of the interaction of the Sb(III) center of $SbCl_5^{2-}$ with a transition metal center. The distance is significantly shorter than the sum of Bondi's van der Waals radii (3.85 Å; r_{Sb}, 2.1; r_{Pt}, 1.75 Å).[36] Bujak and Zaleski have suggested that the radius for Sb in antimony(III) chlorides is about 1.6 Å,[43] which would imply that the Pt···Sb contact lies near the van der Waals limit. The dihedral angle of the coordination planes (defined by the four bonded atoms) for Pt and Sb is 1.4(1)°. The Sb atom is displaced by 0.084 Å out of the coordination plane toward the Pt center, as expected for the presence of a stereochemically active lone electron pair on the Sb(III) center. The Pt···S3 and Pt···Sb vectors form 78.3° and 78.7° angles, respectively, with the platinum coordination plane, which results in an almost linear S3···Pt···Sb chain of atoms (173.57(2)°). When viewed down the Pt···Sb vector (Supporting Information, Figure S4), the four equatorial Sb−Cl bonds are not eclipsed by the

(37) Razak, I. A.; Usman, A.; Fun, H.-K.; Yamin, B. M.; Kasim, N. A. *Acta Crystallogr., Sect. C: Cryst. Struct. Commun.* **2002**, *58*, m162.
(38) Jaschinski, B.; Blachnik, R.; Reuter, H. *Z. Anorg. Allg. Chem.* **1999**, *625*, 667.
(39) Kozawa, K.; Uchida, T. *Acta Crystallogr., Sect. C: Cryst. Struct. Commun.* **1990**, *c46*, 1006.
(40) Bujak, M.; Zaleski, J. *Main Group Met. Chem.* **2002**, *25*, 571.
(41) Zaleski, J. *Ferroelectrics* **1997**, *192*, 71.
(42) Ensinger, U.; Schwarz, W.; Schmidt, A. *Z. Naturforsch., B: Chem. Sci.* **1982**, *37*, 1584.
(43) Bujak, M.; Zaleski, J. *Z. Naturforsch.* **2001**, *56*, 521.

Pt−N or Pt−S bonds; this suggests a tendency to reduce these interactions. The resulting Cl−Sb···Pt−L (L = N, S) torsion angles involving closest Cl/L neighbors range from 12.5(1) to 22.6(1)°. This conformation results in several contacts that are ~0.1 Å less than the sum of van der Waals radii (Cl2···S1, 3.430(2); Cl5···C8, 3.393(6); Cl5···C9, 3.317(5); Cl3···S2, 3.457(3) Å). The shortest contacts involve the mutually trans-positioned Cl2 and Cl5 atoms.

We have scrutinized the structure $[Pt(NO_2phen)(ttcn)](SbCl_5)\cdot 2CH_3CN$ to assess the influence of the Pt···Sb interaction on the cation and anion. The packing indices for the PF_6^- (73.1% when refined without disorder) and $SbCl_5^{2-}$ (73.4%) salts are nearly identical and therefore provide no indication that the conformation of the cation and anion in the $SbCl_5^{2-}$ is a consequence of significantly improved packing efficiency. Aside from some bond asymmetry in the PF_6^- structure discussed above, differences in bond distances of the cations of the PF_6^- and $SbCl_5^{2-}$ salts are largely statistically insignificant. There are, however, four significantly asymmetric bond distance pairs in the $SbCl_5^{2-}$ salt: Pt−S1 (2.2825(11) Å) and Pt−S2 (2.2585(11) Å), C4−C6 (1.420(8)) and C7−C8 (1.470(8) Å), and N1−C5 (1.349(7) Å) and N2−C9 (1.401(8) Å). It seems to be more than coincidence that one bond in each pair involves at least one atom (S1, C8, or C9) that makes a short contact with the anion. Of the 14 non-hydrogen atoms of the phenanthrolinyl group, C9 lies furthest from a best fit plane (0.042 Å), and both C9 and C8 (0.021 Å) are displaced away from the Cl5 atom of the adjacent $SbCl_5^{2-}$. Similarly, the Cl2 and Cl5 atoms of $SbCl_5^{2-}$ are displaced by ~0.06 Å out of a best-fit plane for the equatorial Cl atoms away from the adjacent Pt complexes. (By contrast, S1 and N2 are displaced by 0.03 and 0.04 Å out of the platinum coordination plane toward the $SbCl_5^{2-}$ ion.) The intermolecular interaction involving Cl5 appears to be responsible for a slight shortening of the C8−C9 distance, as compared to C4−C5. Overall, none of the distances and angles of the ttcn ligand lie significantly outside the range observed for structures of other Pt(diimine)$(ttcn)^{2+}$ complexes,[2,3,7] including the PF_6^- and $Sb_4Cl_{16}^{4-}$ salts. However, the resulting S3···Pt−S angles (S1, 82.99(4); S2, 85.91(4)°) are slightly asymmetric, corresponding to a difference of 2.92°, which is significantly larger than the average difference for the nine other structures, 0.67(39)°.

In the $SbCl_5^{2-}$ ion, the equatorial bond lengths (2.5822(13)−2.6531(12) Å) are characteristically longer than the apical Sb−Cl bond (2.4039(11) Å), which is trans to the lone electron pair. Zaleski and co-workers and Bujak and co-workers[40,43−51] have established that the Sb−Cl bond lengths of antimony(III) chlorides are very sensitive to intermolecular interactions, such as hydrogen-bonding and bridging bonds to adjacent metal centers. Large variations in equatorial bond lengths (2.5−3.2 Å) can frequently be rationalized in terms of intermolecular interactions. However, in the present case, we are unable to fully account for the difference, albeit comparatively small, between the Sb−Cl2 distance (2.5822(13) Å) and the three remaining equatorial bond distances (2.6414(12)−2.6531(12) Å). For the purposes of comparison, $[Et_4N](SbCl_5)$ is the best example of essentially isolated $SbCl_5^{2-}$ units where the non-hydrogen contacts exceed the sum of the van der Waals radii.[52] The equatorial (2.605(3), 2.598(3) Å) Sb−Cl distances in that salt are slightly shorter than found for $Pt(NO_2phen)(ttcn)](SbCl_5)\cdot 2CH_3CN$, and the axial Sb−Cl distance (2.346(4) Å) is significantly shorter. On the other hand, the displacement of the Sb atom from the coordination plane (0.074 Å) is comparable to that found for the Pt$(NO_2phen)(ttcn)^{2+}$ salt (0.084 Å). For comparison, we also have identified eight other structures of $SbCl_5^{2-}$ salts in which none of the Cl atoms is involved in a bridging interaction with another Sb atom (i.e., isolated $SbCl_5^{2-}$ units), and the Sb and axial Cl atoms show no evidence of approximately linear H-bonding or non-hydrogen contacts less than the sum of the van der Waals contacts where r_{Sb} was assumed to be 1.6 Å.[43,51−58] For those structures, the average axial Sb−Cl distance is 2.376(17) Å, yet the equatorial Sb−Cl distances range from 2.43 to 2.97 Å. This seems to indicate that intermolecular interactions involving the equatorial Cl atoms have a somewhat limited effect on the axial Sb−Cl distance. Therefore, it would appear that the slight ~0.02 Å elongation in the Pt$(NO_2phen)(ttcn)^{2+}$ salt is a consequence of the Pt···Sb interaction.

The fact that the Pt···S3 distances in the $SbCl_5^{2-}$ (2.9390(12) Å) and PF_6^- (2.9415(15) Å) salts are nearly identical establishes that differences in the apical Pt···S interactions are not responsible for the differences in absorption and emission properties of the two salts. This observation also suggests that the trans-situated Pt···Sb interaction significantly impacts the electronic structure. Previous studies have shown that the apical Pt···S distances for platinum(II) complexes with endodentate ttcn ligands span a range of 2.6−3.3 Å.[3,10,11] The distance is strongly dependent on the σ- and π-donor properties of the ancillary ligands, with strong σ/π-donors (e.g., halides) favoring long distances (3.2−3.3 Å) and weak σ/π-donors (e.g., phosphines) favoring short distances (2.6−2.9 Å). Consequently, values for the subset of seven structurally characterized complexes with diimine ligands fall within a relatively narrow intermediate range (2.81−2.99 Å). The three salts reported here are in excellent agreement with those earlier results. Making use of Pauling's formalism,[59]

(44) Bujak, M.; Zaleski, J. *Acta Crystallogr.,Sect.C: Cryst. Struct. Commun.* **1998**, *54*, 1773.
(45) Bujak, M.; Angel, R. J. *J. Phys. Chem. B* **2006**, *110*, 10322.
(46) Bujak, M.; Angel, R. J. *J. Solid State Chem.* **2007**, *180*, 3026.
(47) Bujak, M.; Zaleski, J. *J. Solid State Chem.* **2004**, *177*, 3202.
(48) Zarychta, B.; Zaleski, J. *Z. Naturforsch., B: Chem. Sci.* **2006**, *61*, 1101.
(49) Zarychta, B.; Bujak, M.; Zaleski, J. *Z. Naturforsch., B: Chem. Sci.* **2007**, *62*, 44.
(50) Bujak, M.; Zaleski, J. *J. Mol. Struct.* **2003**, *647*, 121.
(51) Bujak, M.; Zaleski, J. *Acta Crystallogr., Sect. C: Cryst. Struct. Commun.* **1999**, *C55*, 1775.
(52) Zaleski, J.; Pietraszko, A. *J. Phys. Chem. Solids* **1995**, *56*, 883.
(53) Webster, M.; Keats, S. *J. Chem. Soc. A* **1971**, 298.
(54) Structures refined in the incorrect space group and those without published coordinates also were excluded.
(55) Wismer, R. K.; Jacobson, R. A. *Inorg. Chem.* **1974**, *13*, 1678.
(56) Du Bois, A.; Abriel, W. *Z. Naturforsch., B: Chem. Sci.* **1989**, *44*, 1151.
(57) Derwahl, A.; Robinson, W. T.; House, D. A. *Inorg. Chim. Acta* **1996**, *247*, 19.
(58) Chaabouni, S.; Hadrich, A.; Romain, F.; Ben Salah, A. *Phase Transitions* **2003**, *76*, 1007.
(59) Pauling, L. *J. Am. Chem. Soc.* **1947**, *69*, 542.

and the correlation between the Pt···S3 distance and the displacement of the Pt center from the coordination plane,[2] we estimate the Pt···S3 bond number for the Pt(diimine)(ttcn)$^{2+}$ systems to be 0.2−0.3. There is somewhat conflicting crystallographic evidence regarding the strength of this interaction. For example, in three cases, pairs of Pt(diimine)(ttcn)$^{2+}$ cations have been structurally characterized. For crystals of [Pt(dbbpy)(ttcn)](PF$_6$)$_2$ with different solvates,[2] the Pt···S3 distances (2.965(1), 2.956(2) Å) are nearly identical, as also found for the PF$_6^-$ and SbCl$_5^{2-}$ salts of Pt(NO$_2$phen)(ttcn)$^{2+}$. However, the Pt···S3 distances for the PF$_6^-$ (2.8423(6) Å) and Sb$_4$Cl$_{16}^{4-}$ (2.9944(10) Å) salts of Pt(bpy)(ttcn)$^{2+}$ are substantially different, lying near the edges of the range observed for complexes with diimine ligands. At our current level of understanding, we can only speculate that the short anion−cation contacts in the case of Sb$_4$Cl$_{16}^{4-}$ somehow contribute to this disparity in Pt···S3 distances. In addition, other variations in the Pt···S3 distance within the subset of Pt(diimine)(ttcn)$^{2+}$ structures do not correlate in a predictable manner with the diimine donor properties. For example, Pt(phen)(ttcn)$^{2+}$ (2.821(3) Å) and Pt(5,5′-dmbpy)(ttcn) (2.8532(6) Å; 5,5′-dmbpy = 5,5′-dimethyl-2,2′-bipyridine) have significantly *shorter* distances than their counterparts with electron-withdrawing substituents (NO$_2$phen, 2.9390(12) Å; 5,5′-ditrifluoromethyl-2,2′-bipyridine, 2.956(2) Å).[2] These results contradict the overall trend for platinum(II) ttcn complexes. Though we are unable to advance a detailed explanation for deviations from the larger trend, it is plausible that packing forces can perturb the apical Pt···S distance.

Conclusions

The results presented are illustrative of the impact of the axial Pt···S interaction in Pt(diimine)(ttcn)$^{2+}$ systems on absorption and emission properties. An emerging pattern of evidence is consistent with the suggestion that electron-withdrawing substituents on the diimine ligand stabilize the diimine π^* level and enhance the Pt···S interaction and that these effects contribute to stabilization of states with MLCT character. During investigations of the reaction of Pt(NO$_2$phen)(ttcn)$^{2+}$ with TBPA(SbCl$_6$), we also have encountered the first example of the interaction of a SbCl$_5^{2-}$ ion with a transition metal complex. In the solid state, the Pt···Sb interaction induces a ∼1200 cm^{-1} red shift in the lowest absorption band and a ∼700 cm^{-1} shift in the emission maximum from values obtained for the PF$_6^-$ salt. The fact that the Pt···S3 distances are almost identical for the crystal structures of both [Pt(NO$_2$phen)(ttcn)](PF$_6$)$_2$ and [Pt(NO$_2$phen)(ttcn)](SbCl$_5$)·2CH$_3$CN suggests that the differences in the reflectance and emission spectroscopy are a result of interaction of the metal center with SbCl$_5^{2-}$. These observations suggest stabilization of the lowest MLCT states of the platinum complex, which is consistent with some Sb-to-Pt electron donation. There is considerable precedent for the perturbation of spectra of platinum(II) complexes as a consequence of weak intermolecular interactions at an open coordination site.[11,60−62] For example, we note that the emission maximum for the linear chain Pt(bpy)Cl$_2$ solid shifts by ∼1100 cm^{-1} upon cooling from 300 to 10 K.[63] Over approximately the same temperature range (293−20 K), the Pt···Pt spacing decreases by only 0.08 Å from 3.45 to 3.37 Å.[64] The available spectroscopic and structural information suggests that the Pt···Sb interaction is somewhat weaker than the apical Pt···S3 interaction involving the ttcn ligand. Bearing in mind that SbCl$_5$ is a strong Lewis acid, the findings presented here are consistent with our expectation that the corresponding conjugate Lewis base, SbCl$_5^{2-}$, is weak.

Acknowledgment. Funding for the SMART6000 CCD diffractometer was through NSF-MRI grant CHE-0215950. W.B.C. thanks the National Science Foundation (CHE-0134975) for their generous support and the Arnold and Mabel Beckman Foundation for a Young Investigator Award. S.C. thanks the Cincinnati Section of the English Speaking Union of the United States for a research/travel grant to perform emission and Raman experiments at Département de Chimie, Université de Montréal. We wish to acknowledge the late Prof. Richard C. Elder for helpful discussions. Synchrotron data was collected through the SCrALS (Service Crystallography at Advanced Light Source) project at Beamline 11.3.1 at the Advanced Light Source (ALS), Lawrence Berkeley National Laboratory. The ALS is supported by the U.S. Department of Energy, Office of Energy Sciences, under contract DE-AC02-05CH11231.

Supporting Information Available: Figures S1−S4 and crystallographic data in CIF format for all compounds. This material is available free of charge via the Internet at http://pubs.acs.org.

(60) Falvello, L. R.; Forniés, J.; Garde, R.; García, A.; Lalinde, E.; Moreno, M. T.; Steiner, A.; Tomás, M.; Usón, I. *Inorg. Chem.* **2006**, *45*, 2543–2552.
(61) Song, H.-B.; Zhang, Z.-Z.; Hui, Z.; Che, C.-M.; Mak, T. C. W. *Inorg. Chem.* **2002**, *41*, 3146.
(62) Gliemann, G.; Yersin, H. *Struct. Bonding* (*Berlin*) **1985**, *62*, 87.
(63) Houlding, V. H.; Miskowski, V. M. *Coord. Chem. Rev.* **1991**, *111*, 145.
(64) Connick, W. B.; Henling, L. M.; Marsh, R. E.; Gray, H. B. *Inorg. Chem.* **1996**, *35*, 6261.